

A Tool for Interpretation of Reflood Data and Improvement of Systems Code Models

A. Nagler

Soreq Nuclear Research Center, Yavne, 81800 Israel

J.H. Mahaffy

L.E. Hochreiter

Department of Mechanical and Nuclear Engineering
Pennsylvania State University, University Park, PA 16802

Abstract

Systems codes such as RELAP5, TRAC, and CATHARE have mixed levels of success in reproducing results of reflood experiments. Vapor temperatures measured in the FLECHT SEASET series have been particularly difficult to match. To enhance our ability to isolate and study significant physical phenomena, we have created a multi-field mixed Eulerian-Lagrangian (EL) model. We have focused on the region of dispersed droplet flow above the quench front. The computer program permits any number of Lagrangian droplet fields, providing good resolution of droplet size distributions. All paths of energy transfer between vapor, droplets, rods, and grid spacers have been included in the model. In addition a model has been included for droplet shattering at grid spacers, which provides automatic generation of new droplet fields at each grid spacer. Inclusion of the shattering model was a key component in obtaining an excellent match to FLECHT data. Understanding of all contributions to the problem has given us the ability to produce a model with a level of detail appropriate for systems codes. A new set of well instrumented reflood experiments is underway at Penn State. We expect further improvements in modeling capability as we apply the detailed EL model to the interpretation of results.

1. Introduction

After many years of research into the reflood process, high fidelity simulation of core reflood remains elusive. Basic phenomena associated with reflood have been studied extensively with many separate effects and integral experiments. Very basic analysis by researchers such as Andreani and Yadigaroglu [1] has also increased our understanding. However, attempts to capture this knowledge in the models, used by safety analysis tools such as RELAP5 [2], TRAC[3], or CATHARE[4], have at best achieved mixed results. Typical shortcomings include poor prediction of the quench propagation above the core mid-plane, and poor predictions of vapor temperature above the quench front.

The goal of our research has been to understand and assess physical models and correlations in a

context that is directly applicable to best estimate safety codes. Our work has been restricted to the dispersed film boiling regime in the upper core which controls the vapor temperature and sets the stage for the late term quench propagation. Since most reflood experiments are quasi-steady, we have used steady state flow equations, Eulerian for the vapor flow and Lagrangian for the droplets. We have taken care to account for all paths of energy flow between heater rods, grid spacers and both fluid phases. Effects of grid spacers on droplet size are also included. These spacer models have the largest impact on our ability to match data from FLECHT SEASET.

2. Basic Flow Equations

The assumptions for our model are divided into three categories: system, vapor, and droplets.

System:

- C Quasi-steady-state: the velocity of the quench front is very small compared to the droplet and vapor velocities. Thus, we can consider the quench front as a stationary continuous source of droplets supplying a steady state distribution of droplets at the entrance.
- C 1D analysis: axial changes are much larger than the lateral variations. We note that the spacer grids have the same height across the core. The constriction effect of the spacer grid is then uniform in the transverse dimension. Hence, we can neglect the effect of the surrounding channels.
- C Fluid pressure: the dispersed droplets are incompressible and have pressure equal to that of the gas.
- C Pressure drop along the channel: experimental observations of FLECHT SEASET show that the pressure is quite uniform along the channel; e.g., in run 31504, a change of only 0.02 bar was observed between 1.83 m and the exit (Unal et. al., 1994). Due to this observation, the vapor momentum equation can be neglected (Andreani et. al., 1997).

Vapor:

- C Vapor viscosity: the vapor is compressible but inviscid except at the droplet interface.

Droplets:

- C Modeling droplets: the volume occupied by droplets is insignificant ($\alpha > 0.99$) as far as considerations of gas dynamics are concerned. This means that the droplets are regarded as volumetric sources of mass, momentum, and energy for the vapor phase but are not modeled as a continuum.
- C Spherical droplets: the droplets are assumed to be spherical. This assumption is verified by the small Eotvos number.
- C Droplets at saturation: this is based on the general observation that water approaching a quench front is saturated, which allows deleting the energy equation for droplets.
- C Two phase interaction: transfer of mass (evaporation), heat, and momentum occurs between droplets and vapor.
- C Droplet break-up: droplets break up only by collision with the spacer grid. Break-up of droplets in between the spacer grids is ignored. This is verified by the small Weber numbers.
- C Droplet coalescence: coalescence is ignored due to the very high void fraction.
- C Wall temperature: the wall temperature is above the Leidenfrost temperature, 550-600 K. Consequently, impingement of droplets on the wall may occur only for vigorous flow.

A 1-D staggered mesh typical of safety codes is used (Figure 1), to construct the finite volume method for the Eulerian flow equations. The resulting steady state vapor mass and energy equations are:

$$(a \rho_v u_v A)_{k+1/2} - (a \rho_v u_v A)_{k-1/2} = G \quad (1)$$

$$\begin{aligned} & [(a \rho_v u_v e_v + a u_v P) A]_{k+1/2} - [(a \rho_v u_v e_v + a u_v P) A]_{k-1/2} \\ & = G h_f + q_{c,w2v} - q_{rad,v} \end{aligned} \quad (2)$$

where

k - control volume index;

a - vapor void fraction;

ρ_v - vapor density [kg/m³];

u_v - vapor velocity [m/s];

A - subchannel cross section area [m²];

G- evaporation rate (from a heat conduction limited model) [kg/s] ;

e_v - specific vapor internal energy [J/kg];

P - system pressure [bar];

h_f - liquid saturation enthalpy [J/kg];

$q_{rad,v}$ - net radiation heat absorbed in the vapor [W];

$q_{c,w2v}$ - convective heat transfer from rod walls to the vapor [W].

Upwind averaging is used to obtain quantities required at the volume edges. For positive vapor velocities this means that:

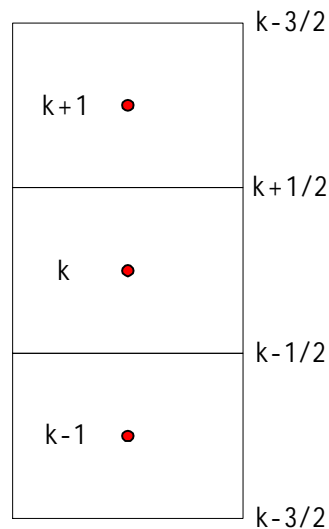
$$\begin{aligned} & (a \rho_v u_v A_c)_{k+1/2} = (a \rho_v)_{k+1} (u_v A_c)_{k+1/2} \\ & (a \rho_v u_v A_c)_{k-1/2} = (a \rho_v)_k (u_v A_c)_{k-1/2} \end{aligned} \quad (3)$$

The droplet size distribution at the starting elevation (mid-plane) is taken from data. Our model represents this distribution by permitting any number of representative droplet size groups. The number of droplets in each group is determined by the initial distribution. The starting velocity of each group is taken from data. The trajectory of each group is obtained from a simple motion equation:

$$\frac{du_i}{dt} = 0.75 \left(\frac{C_{D_i}}{D_i} \right) \left(\frac{\rho_v}{\rho_d} \right) |u_{v,i}| u_{v,i} + g \quad (4)$$

where $u_{v,i}$ is the relative velocity between the vapor and the i^{th} size group. The change in diameter associated with each group is determined from conservation of mass for the group:

$$\frac{dm_i}{dt} = G \quad (5)$$



Inlet Boundary Conditions:

Vapor (T_v, U_v, m_v)

Droplets ($T_s, U_{di}, D_{di}, n_{di}, m_{di}$)

Figure 1. Computational mesh points and control volume notations

where \dot{G} is phase change rate for the i^{th} size group. Droplet energy is controlled by the assumption that the droplets are at the saturation temperature. Number density of a given group in each Eulerian volume is determined by balancing the number per second into each volume with the number per second out.

The coupled equations for steady flow are solved by an iterative procedure described in detail by Nagler[5].

3. Models for Momentum and Heat Transfer

The drag coefficient used in Eqn. 4 is a fairly standard expression for drag on a sphere, altered to include a “blowing” factor to adjust for the effects of boiling. It is estimated in two regions according to the vapor-to-droplet Reynolds number (Paik et. al. [6]).

$$C_{D,i} = \begin{cases} \frac{24 (1.0\% 0.1 Re_i^{0.75})}{Re_i (1.0\% B)^{0.2}} & Re \sim 1000 \\ \frac{0.44}{(1.0\% B)^{0.2}} & Re \gg 1000 \end{cases} \quad (6)$$

where, i represents the group of droplets having a given diameter, and the blowing factor is:

$$B = \frac{h_v \& h_{sat}}{h_{fg}} \quad (7)$$

The interfacial heat transfer coefficient is based on the Lee-Ryley correlation, including a blowing factor adjustment for boiling.

$$Nu_d = \frac{(2.0\% 0.74 Re_i^{0.5} Pr_v^{0.333})}{(1.0\% B)^\beta} \quad (8)$$

The exponent “ β ” used for the blowing factor correction was found to best match the data for FLECHT SEASET test 31504 when set to 2. This is higher than used for normal models, and may reflect extra boiling induced by the close proximity of rods, or the general need for a larger Nusselt number.

For wall-to-vapor convective heat transfer, we considered three options. The first is the well known Dittus-Boelter equation for smooth pipes. The second one uses a heat transfer correlation of the square rod bundle geometry with a pitch-to-diameter ratio of 1.33 developed by Wong and Hochreiter [7]. The third option, is a simpler single range Wong-Hochreiter [7] correlation.

$$h_{v,1f} = 0.0797 Re_v^{0.6774} Pr^{0.333} \quad (9)$$

This is the correlation that we found most appropriate for FLECHT SEASET test 31504. And was augmented for the presence of droplets, and grid spacer entrance effects (see Ref. [5] for details).

For test 31504, rod temperatures in the upper portion of the bundle are low enough to permit cooling by droplet contact. The heat transfer coefficient, $h_{dc,w2d}$, is calculated with the enhanced Forslund-Rosenow correlation, as proposed for a void fraction greater than 0.8 by Bajorek and Young [10].

$$h_{dc,w2d} = \begin{cases} 0.0 & \text{if } Re_v < 4000 \\ 0.00638 (Re_v \& 4000)^{0.6} (1 \& a)^{2/3} \left[\frac{k_v^3 h_{fg} g \rho_d \rho_v}{(T_w \& T_d) \mu_g D_d} \right]^{0.25} & \end{cases} \quad (10)$$

Temperatures in the upper core can be high enough that radiative heat transfer must also be considered. We have adapted the model from TRAC-B [10], which calculates rod to liquid, rod to vapor, and rod to rod energy transfer. Radiation transfer between rods and grid spacers was also modeled.

4. Grid Spacer Effects

Results in the next section will demonstrate that modeling of droplet shattering is critical to obtaining good vapor temperature predictions. When droplets of a specific diameter group collide with the spacer grid edge, they are shattered into a new spectrum of droplet sizes. To avoid tracking an excessive number of droplet groups, we represent this spectrum through the creation of a single new diameter group for each group reaching the grid spacer. Some droplets pass through untouched by the spacer, so the original size group must be maintained with an appropriate reduction in droplet number density. The ratio of diameters between the shattered and incoming droplets depends on the incoming Weber number. The appropriate Weber number is:

$$We_{0i} = \frac{\rho_d V_{d,i}^2 D_i}{s} \quad (11)$$

where,

- We_{0i} - Weber number of group 'i' approaching to the spacer grid
- ρ_d - droplet's liquid density [kg/m^3]
- $V_{d,i}$ - droplet velocity of group 'i' [m/s]
- D_i - droplet diameter of group 'i' [m]
- s - droplet surface tension [N/m].

The average diameter of the shattered droplets is calculated using a correlation developed by Yao, et al. [10]. The correlation is divided into several regions depending on the ratio between the incoming droplet diameter and the spacer grid width.

$$D_{\text{new}} = \begin{cases} \frac{12.0}{Ek_{2\text{surf}} @ We_0} @ D_0 & \text{for } \frac{D_0}{w_{\text{sg}}} \# 3.5 \\ 3.05 @ We_0^{(0.46)} @ D_0 & \text{for } 3.5 < \frac{D_0}{w_{\text{sg}}} \# 4.0 \\ We_0^{(0.2)} @ D_0 & \text{for } \frac{D_0}{w_{\text{sg}}} > 4.0 \end{cases} \quad (12)$$

where:

- $Ek_{2\text{surf}}$ - fraction of droplet kinetic energy that transformed into surface tension.
- D_0 - diameter of incoming droplet.

Yao et al. estimate that about 15% of the kinetic energy of the incoming droplet converts to the surface energy of the generated small droplet.

Grid spacers also have the potential to alter the droplet size distribution by de-entraining droplets onto a liquid film, and re-entraining droplets with a different mean diameter at the trailing edge of the

space. For FLECHT SEASET test 31504 all grid spacer were hot enough that a liquid film could not form on the spacers.

Care was taken to model the impact spacer grids on heat transfer. Models were included to determine spacer grid temperature based upon conduction and radiation from the rods, and convective and radiative heat transfer with the two fluid phases. Change in flow geometry at the grid spacers was also fed to the rod heat transfer models. Rod heat transfer was altered at the spacers do to a change in vapor velocity and a change in the effective hydraulic diameter. Rod heat transfer immediately downstream of the grid spacer was enhanced to account for local enhancement of turbulence. For the test 31504, the energy path from rod to spacer to fluid had no significant impact on results. However, the impact through flow geometry changes was significant.

5. Results for FLECHT SEASET 31504

Figure 2 compares computed vapor temperature versus data for three different analyses. The base analysis started with 14 diameter groups to represent the inlet droplet distribution, and doubled the number of groups at each grid spacer (solid vertical lines in Figure 2), resulting in a total of 112 droplet groups at the top of the bundle. The second calculation started with a single droplet group with the inlet Sauter mean diameter, and again doubled the number of groups at each spacer. This calculation missed the total evaporation of smaller drops predicted at the top of the bundle by the first calculation, but generally followed detailed results quite well. The third calculation simply follows a single droplet group through the bundle, without shattering at grid spacers.

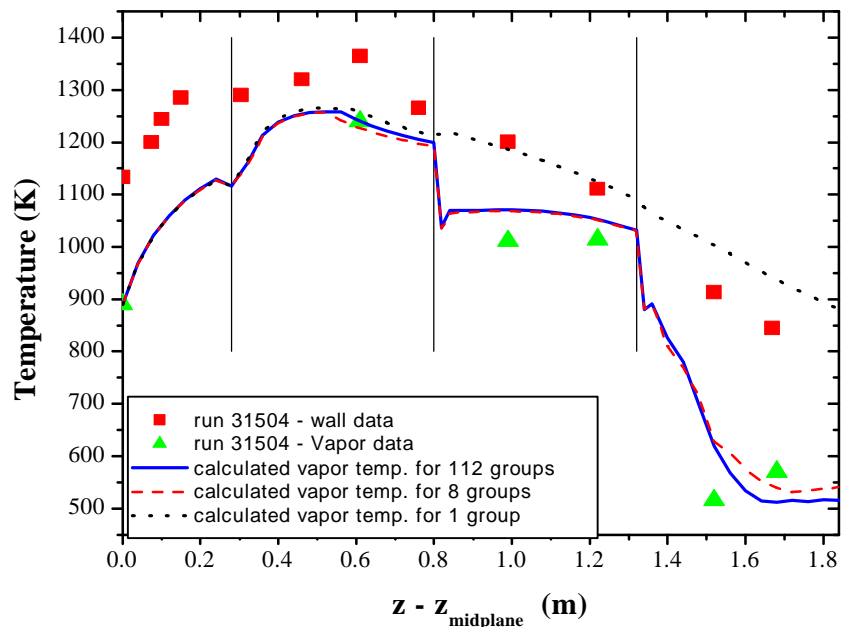


Figure 2. Vapor temperature for single and multiple groups along the channel

At the entrance of the second spacer grid, the temperature drop is more significant than at the first one. At this point the velocities of the droplets have increased sufficiently that shattering becomes more effective. Shattering leads to a larger liquid surface area, boosting evaporation. At the third spacer grid, the breakup of droplets continues to be the dominant process. Many groups shatter into spray due to the higher droplets' velocity. Most of the new groups evaporate completely very quickly. The temperature continues to drop even beyond the direct vicinity of third spacer grid, which is in contrast to the behavior at the first two spacer grids. The change in behavior is related to the increase of the evaporation rate due to direct contact heat transfer from wall to droplets, and is also influenced by a reduction in the blowing factor.

Some analyses of this experiment ignore the data points for vapor temperature plotted in Figure 2 at 1.5 and 1.7 meters above the mid-plane. These are valid data points and indicate a strong cooling driven by phase change. A sensitivity study with our model showed that direct droplet cooling of the rods was necessary for predicted results to come close to these data points. The effects of shattering on the third grid spacer, even with reasonable variations on our model, do not produce enough vapor cooling.

Figure 3 presents quality computed in the three runs described above and qualities taken from the 31504 test report. The close match suggests that we are getting right mix of droplet boiling and direct heat transfer to the vapor.

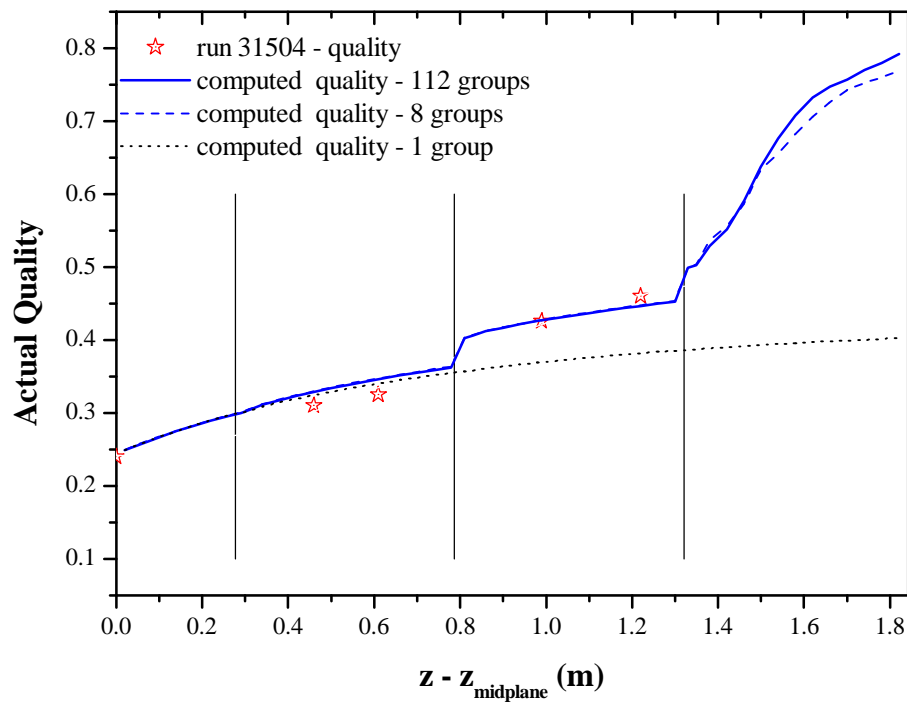


Figure 3. Actual quality for single and multiple groups along the channel

6. Conclusions

Our Eulerian-Lagrangian modeling approach accounts for all processes contributing to mass and energy transfer, within a relatively simple modeling framework. For FLECHT SEASET test 31504, it has resulted in remarkably good comparisons between calculation and data. A new set of USNRC sponsored reflood experiments are starting soon at Penn State University with more detailed data than was available from the FLECHT SEASET series. In particular we will have many more vapor temperature measurements available to us. This analytic tool will be applied to aid in understanding the new data, to check existing correlations against the data, and where necessary aid in the development of new correlations.

We are also using this tool to explore potential model improvements for the USNRC consolidated reactor safety analysis code [11]. Conclusions reached from the Eulerian-Lagrangian reflood analysis on interfacial and wall heat transfer correlations will have direct value to the consolidated code. Use of the knowledge gained on modeling of droplet shattering will require a little more work to adapt to the Consolidated Code. We would prefer not to operate the consolidated code with eight or more droplet fields to account for droplet shattering. However, a single area transport equation has already been adapted to the Consolidated Code [12]. We are currently using our Eulerian-Lagrangian code to develop and justify an approach to modeling droplet shattering within the context of a single area transport equation.

References

1. Andreani A. and Yadigaroglu G., "A 3-D Eulerian-Lagrangian model of dispersed flow film boiling including a mechanistic description of the droplet spectrum evolution- I. The thermal-hydraulic model," *Int. J. Mass Transfer*, 40, pp. 1753-1772, 1997.
2. RELAP5/MOD3 Code Manual, Vols. 1-6, Idaho National Engineering Laboratory Report, INEL-95/0174, US Nuclear Regulatory Commission Report, NUREG/CR-5535, 1995.
3. TRAC-PF1/MOD1: An advanced best-estimate computer program for pressurized water reactor thermal-hydraulic analysis, Los Alamos National Laboratory Report, LA-10157-MS, US Nuclear Regulatory Commission Report, NUREG/CR-3858, 1986.
4. Bartak, J. and Haapalehto, T., "Simultaneous bottom and top-down rewetting calculations with the CATHARE code," *Nuclear Technology*, 106, pp. 46-59, 1994.
5. Nagler, A. "An Eulerian Lagrangian Simulation of the Dispersed Flow Film Boiling Regime During Reflood Including the Spacer Grid Effects," Pennsylvania State University PhD. Thesis, August 2000.

6. Paik, C. Y., Hochreiter, L. E., Kelly, J. M., and Kohrt, R. J., "Analysis of FLECHT-SEASET 163 Rod Blocked Bundle Data Using COBRA-TF," NUREG/CR-4166, 1985.
7. Wong, S., and Hochreiter, L.E., "Low Reynolds Number Forced Convection Steam Cooling Heat Transfer in Rod Bundles," Westinghouse Report, 80-WA/HT-59, 1980.
8. Bajorek, S. M., and Hochreiter, L. E., "Prediction of reflood behavior for tests with differing axial power shapes using WCOBRA/TRAC," HTD-Vol. 165, Numerical Modeling of Basic Heat Transfer Phenomena in Nuclear Systems, ASME, 1991.
9. Borkowski, J. A., Wade, N. L., Rouhai, S. Z., Shumway, R. W., Weater, W. L., Retting, W. H., Kullberg, C. L., " TRAC-BF1/MOD1 Models and Correlations," NUREG/CR-4391, 1992.
10. Yao, S. C., Hochreiter L. E., and Cai K. Y., "Dynamic of droplets Impacting on Thin Heated Strips," J. of Heat Transfer, 110, pp. 214-220, 1988.
11. Mahaffy, J. H., Uhle, J., Dearing, J., Downar, T., Johns, R., and Murray, C., Architecture of the USNRC Consolidated Code, 2000a, Proceeding of ICONE 8, 8th International Conference on Nuclear Engineering, Baltimore, MD USA, April 2-6, 2000.
12. Ishii, M. Kim, S. and Uhle, J., "Interfacial Area Transport: Data and Models," CSNI Workshop on Advanced Thermal-Hydraulic and Neutronic Codes: Current and Future Applications," Barcelona, Spain (April 2000).